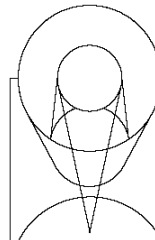




TECHNICAL REPORT



SPACE
TELESCOPE
SCIENCE
INSTITUTE

Operated for NASA by AURA

Title: Calibrating MEMS-based multi-object spectrographs: lessons learned from the experience with IRMOS at Kitt Peak	Doc #: JWST-STScI-001574, SM-12 Date: October 29, 2008 Rev: -
Authors: M. Robberto, J. MacKenty Phone: 410 – 338 - 4382	Release Date: 10 February 2009

1.0 Abstract

This report deals with the calibration of the astronomical spectra taken with IRMOS, the only existing spectrograph based on MEMS devices and the closest precursor of NIRSPEC. After illustrating the main instrument features, we show that the IRMOS calibration strategy requires minimal use of the DMD and grating wheel, and does not assumes an instrument model. The calibration is done “on the fly” immediately after the science frames, with the instrument exactly in the same configuration used to take the science data seconds before. Regardless of the differences in requirements, design, performance and operating environment between IRMOS and NIRSPEC, the experience with IRMOS may provide useful hints on how to operate NIRSPEC, at least in the early commissioning phases before the instrument gets fully characterized.

2.0 Introduction

Among the instruments to be installed on the JWST, the IR spectrograph NIRSPEC is the one posing the major calibration challenges. This because of the novel design of the instrument, which uses MEMS devices (Micro-Shutter Arrays, MSAs) as a rapidly reconfigurable slit device. NIRSPEC will be the first instrument of this type to be used in space and will leverage on extremely limited experience on the ground: there is only one spectrograph based on MEMS devices, IRMOS, currently offered to the astronomical community at the Kitt Peak National Observatory. Despite the fact that IRMOS uses a different type of MEMS (Texas Instrument DMD “micromirros” vs. MSAs) and operates on the ground, it still represents a unique test bench for MEMS based instruments. Considering that IRMOS was originally conceived as a demonstrator for the JWST spectrograph, a report on the “lessons learned” with this instrument, in particular in what concerns the calibration procedures, appears timely and appropriate.

Operated by the Association of Universities for Research in Astronomy, Inc., for the National Aeronautics and Space Administration under Contract NAS5-03127

Check with the JWST SOCCER Database at: <http://soccer.stsci.edu/DmsProdAgile/PLMServlet>
To verify that this is the current version.

3.0 IRMOS

IRMOS (InfraRed Multi-Object Spectrograph) represents the first attempt to build a multi-object spectrograph based on MEMS technology. The origin of IRMOS is strictly associated with JWST. The first concept was proposed in the development phases of JWST in early 1996 (MacKenty & Stiavelli 2000). NASA subsequently funded the Pre-Phase A study of the instrument, as well as an independent development of enabling MEMS technology (MacKenty et al. 2000). The instrument design started in 1998, and delivery at Kitt Peak National Observatory (KPNO) occurred in September 2004, where it is now successfully operated and offered to the astronomical community as a facility instrument.

A number of papers deal with different aspects of IRMOS design, in particular cryogenic mechanisms (Shepis et al. 2003), optical design (Winsor et al. 2000), fabrication of the optical parts (Ohl et al. 2003), laboratory testing (Ohl et al. 2004) and commissioning (MacKenty et al. 2006). We will therefore not provide here a full description of the instrument, listing only a few facts relevant to the data reduction strategy:

1. The reconfigurable slit device is a Texas Instrument (TI) 848×600 elements Digital Micromirror Device (DMD). Each DMD element is a micromirror (17 micron center-to-center) which may be tilted along its diagonal by $\pm 10^\circ$.
2. The detector (Focal Plane Assembly, FPA) is a Rockwell (now Teledyne) Hawaii-I HgCdTe device of 1024×1024 pixels sensitive between 0.8 and 2.5 micron. The physical pixels size is 18.5 micron.
3. The pre-DMD optics delivers, at the KPNO 4m Mayall telescope, 0.2 arcsecond per micromirror. The post-DMD optics has a 1:1.09 magnification on the detector, which therefore maintains nearly the same 0.2 arcsec/pixel nominal scale of the DMD. The scale nearly doubles (0.4 arcsec/pixel) at the KPNO 2.1 m telescope. The scale intentionally samples the angular or spectral resolution element with 3-5 pixels. Oversampling facilitates dealing with distorted data, both in spatial and spectral direction. Note that NIRSPEC, on the other hand, generally undersamples the PSF on the MSA plane.
4. The field of view on the detector is limited by the DMD size to 170×120 arcsecond at the 4 m telescope, twice this value at the 2.1 m telescope.
5. The calibration subsystem intercepts the incoming beam from the telescope and injects, through a retractable flat screen, the light projected either by continuum or line lamps located in the immediate vicinity of the screen.
6. IRMOS operates in double correlated sampling readout mode, i.e. a first read is taken immediately after a detector reset followed by a second one at the end of the integration; a single extension fits file containing the difference of the two reads is therefore produced for each observation.

For the coming discussion, it is also important to be aware of a few issues that affect this novel instrument as they impact the data reduction strategy.

- Thermal background. The IRMOS optical design, fully based on off-axis reflective optics, does not allow for a light tight cold chamber separated by the external environment only through a cold stop at the pupil. The detector, sensitive up to 2.5micron, therefore sees diffuse thermal radiation. The intensity of the thermal background varies across the detector field, reaching at one extreme of the field high enough values to prevent scientific observations. The background pattern is quite stable over time and can be easily subtracted out (of course, the loss of sensitivity remains). A cold focal plane mask has been inserted in 2006 in the vicinity of the detector which substantially reduces the amount of stray light falling on the detector. The data presented in this report have been taken *before* the installation of this cold mask
- DMD defects. The DMD device installed in IRMOS is based on mid'90s TI technology and does not benefit from the great improvements made by TI in the last 10 years in terms e.g. of size, contrast, and device reliability. In particular, a few mirrors of the IRMOS DMS have become non functional over the years, two in particular have developed an anomaly in their circuitry which makes them emit a bright continuum LED-type light. They fall at intersection of rows and columns which also appear to be in part non-functional. One of the LEDs mirrors falls in the high background area of the field and therefore does not further degrade the overall field coverage of the instrument. The other is in the useful low-background part of the field and makes a few columns unusable. It provides, on the other hand, an excellent reference point for the alignment of the DMD mirrors (see next Section).
- Grating wheel. The grating wheel, controlled through a stepping motor, does not reposition itself with enough accuracy to preserve the pixel-to-pixel mapping between the DMD and detector. This was an accepted part of the IRMOS design, on the basis of the estimated gravity vector variation (i.e. instrument internal flexures) with time. The repositioning error affects the alignment procedure of the slit on the celestial sources, as an iterative solution has to be adopted based on the initial approximate map and on the position in the field of a defective LED mirror. This also affects the wavelength calibration procedure, which must take into account the inability of the optical system to return in a well defined status.

4.0 Dataset used for the present report

The data used for the present study are relative to an early commissioning run of IRMOS, on the night of September 16, 2005. The instrument was installed at the KPNO 2.1m telescope and the optical layout at that time did not include the cold focal plane mask that has been installed more recently to reduce the amount of thermal background on the detector. Whereas the data are not representative of the current instrument performance, they still provide a good illustration of the calibration methods generally adopted with the instrument.

5.0 IRMOS Operations: Initial Calibration

5.1 DMD-FPA calibration

For MEMS based spectrographs the most important preliminary calibration step is the mapping of the DMD on the FPA: to open or close a certain DMD, we must know how to transform FPA pixels into micromirrors and viceversa. For convenience, we shall use hereafter the term “mirror” and “slit” as synonyms. Accordingly, “mirror in the ON status” and “open slit” have the same meaning.

The strategy we have adopted is to generate a regular grid (m_x, m_y) of mirrors “open” on the DMD, illuminate them and measure the centroids of their images on the FPA. This requires the grating wheel to be positioned with the imaging mirror in the optical path. The grid of positions commanded to the DMD is made by 3x3 apertures separated by 100 elements, center-to-center, on a rectangular grid (Figure 1a). The grid of open apertures is then illuminated with white light, and a few seconds of exposure are sufficient to acquire the image shown in Figure 1b.

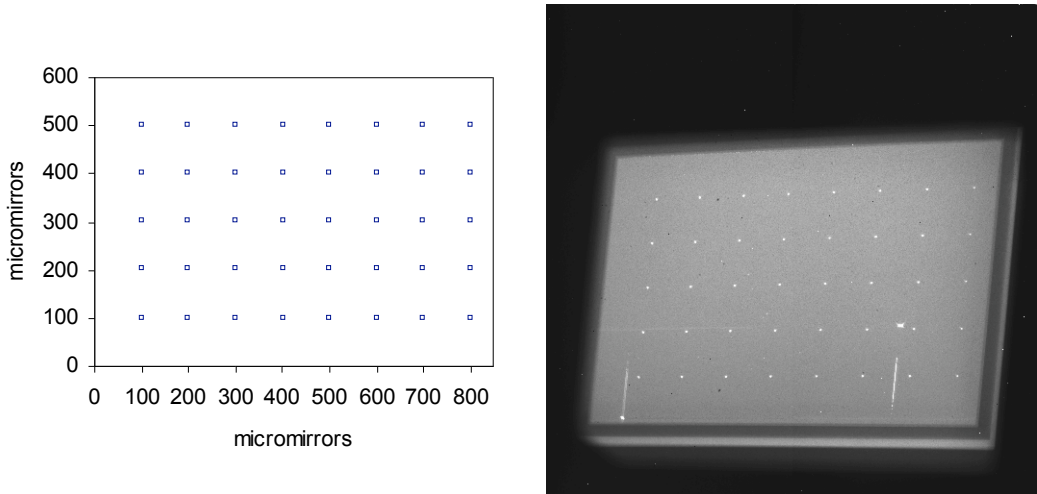


Figure 1: The pattern of mirrors commanded in the ON position on the DMD (left) and the corresponding image on the full detector field(right);

Figure 1 shows the position of the corresponding points (p_x, p_y) on the detector. The field seen by the DMDs fills only ~50% of the detector area. Also, due to the off-axis optical design, the field imaged by the DMD is skewed and distorted.

In order to find the centroids of the spots, one has to subtract the non-uniform background, correct for flat field and remove the spurious features. Instead of applying a series of calibration passages, we simply shift the pattern by $\frac{1}{2}$ of the width of the pattern (50 elements) in both directions and take another image (Figure 2).

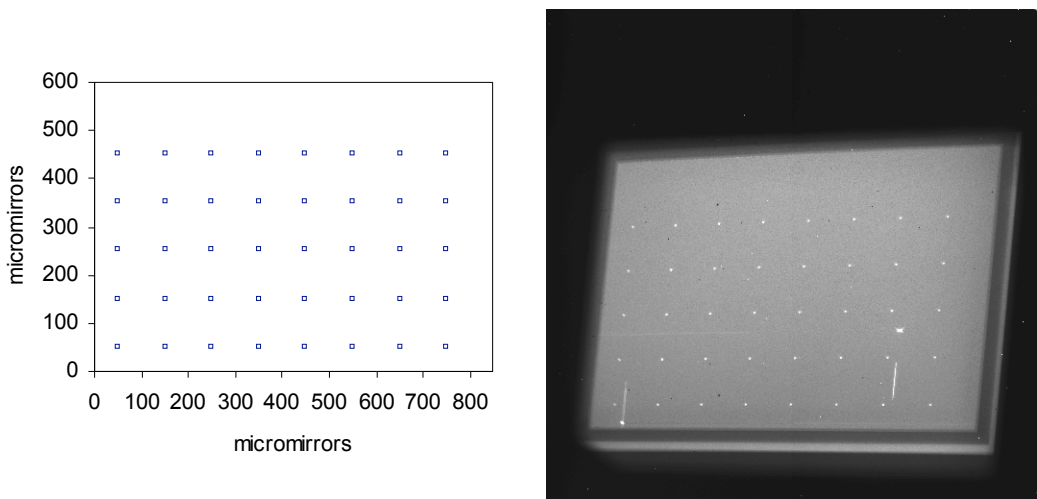


Figure 2. The same pattern of Figure 1, shifted by $\frac{1}{2}$ of the width of the pattern in the bottom-left direction.

The two images can then be subtracted and the absolute value taken, producing the image shown in Figure 3.

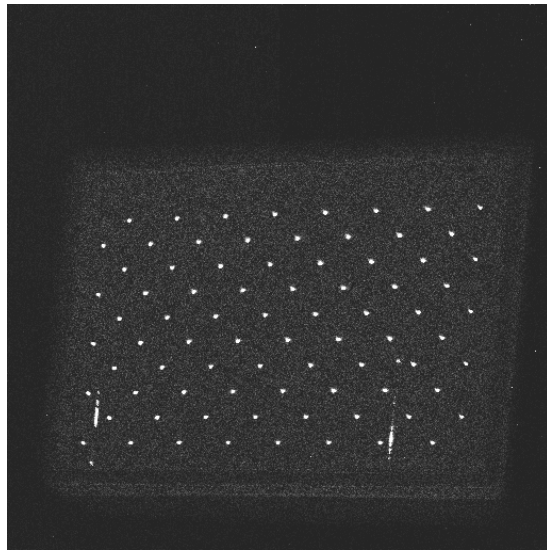


Figure 3. Difference between the images shown in Figure 1 and Figure 2, right.

An IDL routine is then used to find the centroids and calculate the transformations from the DMD to the FPA and vice-versa (Figure 4). In our case, the solution is accurate to within a fraction of a pixel, which is sufficient for IRMOS. To improve the accuracy, one has a choice of strategies:

- a) use a denser grid,
- b) calculate a higher order solutions,
- c) correct for flat field.

Check with the JWST SOCCER Database at: <http://soccer.stsci.edu/DmsProdAgile/PLMServlet>
To verify that this is the current version.

The routine should automatically associate a centroid to a DMD position. Therefore, one has to specify an initial search position and radius on the detector for each open spot. The search parameters must be accurate enough to avoid confusion between adjacent spots. If the image distortion is large or the grid too dense, a simple search pattern based on a rectangular matrix may provide wrong associations. To unambiguously identify each spot, one may therefore have to start either with some manual fine tuning to the search grid or a previously calculated solution.

In principle, the DMD-FPA mapping should be a constant of the instrument, at least within each cooling cycle. As anticipated in Section 3, this is not the case for IRMOS. In the next section we explain how to mitigate this problem.

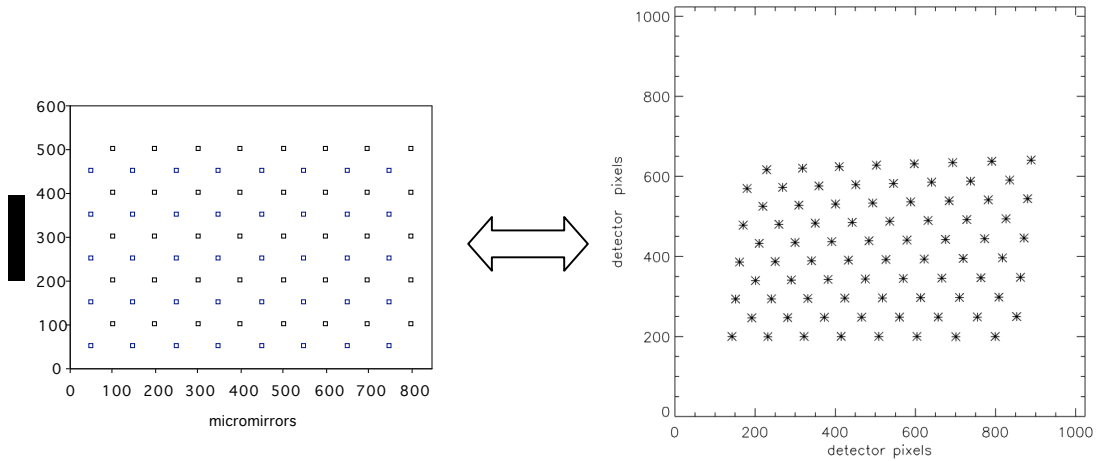


Figure 4. The DMD (left) and FPA (right) patterns used to derive the transformation.

5.2 Stability of the DMD-FPA calibration

The DMD-FPA map is valid for a given alignment of the optical elements between the two corresponding focal planes, in particular of the imaging mirror in the moving grating wheel. As anticipated in Section 3, this is not the case with IRMOS¹.

This has two major consequences:

1. When a field is imaged, the DMD-FPA map stored in the memory is typically no longer valid. To turn ON/OFF a mirror at the location (m_x, m_y) one has to use a transformation different from the stored $(m_x, m_y) = T(p_x, p_y)$ transformation.
2. When a spectrum is taken, i.e. the grating wheel is rotated to insert a diffraction grating in the optical path, the map between the ON mirror and wavelengths seen

¹ The grating position repeatability is also a concern for NIRSPEC (T. Beck, priv. comm.).

on the detector varies randomly. In this case the transformation can be represented as $\lambda(m_x, m_y) = \Lambda(p_x, p_y)$, with the application Λ poorly defined.

Problem 1 is solved by finding a correction to the map. Since the typical displacement of the grating wheel produces a shift of the reimaged field mostly in the vertical direction, one can assume that, to a first order approximation, it is

$$(m_x, m_y) = T(p_x, p_y) + D_y .$$

The offset parameter D_y can be readily estimated by measuring the distance between the actual and expected position of an open slit on the FPA, or measuring the position of the bright LED spot, which being fixed on the DMD provides a convenient reference point for the projection of the DMD on the detector. On the other hand, due to image distortion, a simple offset in the y direction only is not sufficient to fully account for the position error across the entire field. For targets far from the source used as reference to derive the D_y offset, some iteration is therefore usually needed to find the corresponding slit position, both in y and in x directions.

The second problem is simply solved by performing the wavelength calibration before moving the grating wheel.

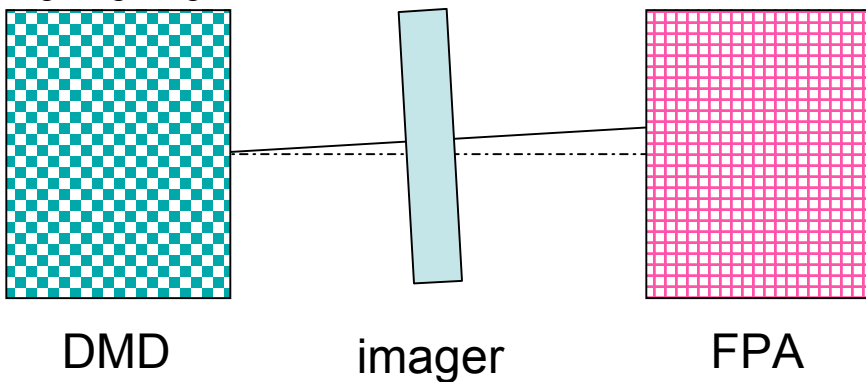


Figure 5.The misalignement of an optical component between the DMD and the detector makes the transformation map no longer valid.

6.0 Target Acquisition

The first step of the data acquisition is the acquisition of a field image (Figure 6). For target acquisition with IRMOS, one usually takes a broad-band image with integration time long enough to directly detect the target. Adjusting the intensity thresholds of the displayed image normally allows for direct visualization of the targets without image pre-processing.

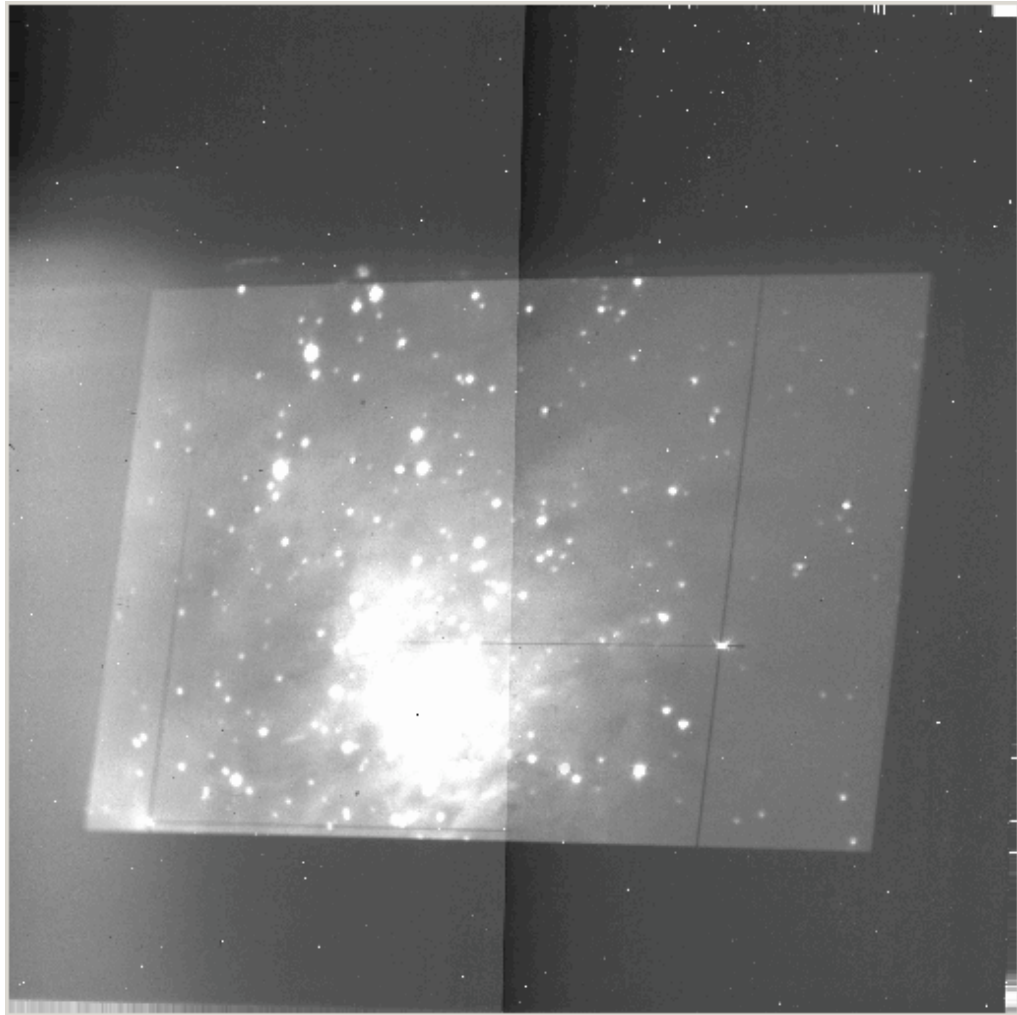


Figure 6. Field centered on the Becklin-Neugebauer object in the Orion Nebula, as seen at the KPNO 2.1m telescope. The field of view is approximately 7×4 arcmin.

Once the image has been taken, a default slit size is defined (e.g. 20 pixel long, 3 pixel wide). By clicking on the displayed image (in pixels), one defines the central location of the slit on the DMD (in micromirrors). Of course, this is where the correct transformation between detector and DMD should be applied. The size of each slit can be individually fine tuned.

One of the most powerful capabilities of MEMS devices is the possibility of creating and “inverted” slit pattern, where the slits are actually set to the OFF position and the rest of the field is in the ON position. This allows refining the target pick-up in “coronographic” mode: instead of moving the slit by small steps, taking an image and measuring the intensity of the flux as usually done with slit spectrographs, the slit is directly displayed against the source PSF leaving the wings visible. This easily allows to fine tune the slit position balancing the intensity of the wings (Figure 7).

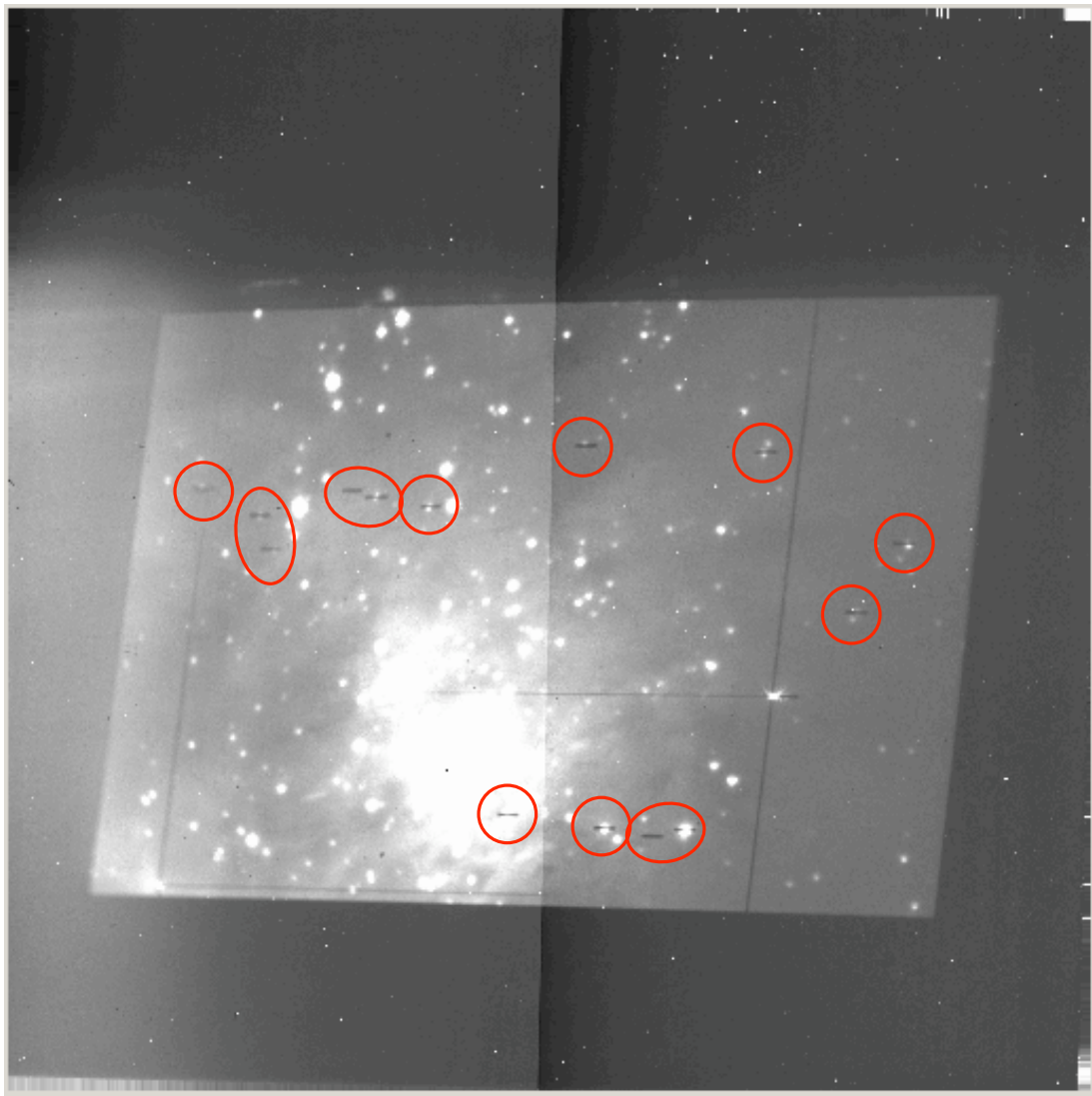


Figure7.The same field of Figure 6, with a set of DMD on the OFF state (red circles) aligned on the target sources.

In principle, fine tuning should not be necessary if the transformation DMD-FPA is accurate and stable enough. As we anticipated in Section 4.2, fine tuning is needed because of the positioning error of the grating wheel of IRMOS.

Once the slits have been aligned on the targets, the entire DMD pattern is inverted and the slits now appear as regular openings. Figure 8 shows the field with the slits in their ON position and the rest of the field in the OFF position. Note the presence of the defective LEDs mirrors (yellow diamonds), of the higher background on the left side of the field and of the bright Trapezium stars (cyan circle) leaking through the DMD field. The Trapezium is visible partially because of the contrast of this DMD device, which has been estimated around 300 (against a value >2500 reported for the last generation of

DMDs) and partially because of latency of the bright source images on the detector. Our data do not allow further discriminating between the two processes.

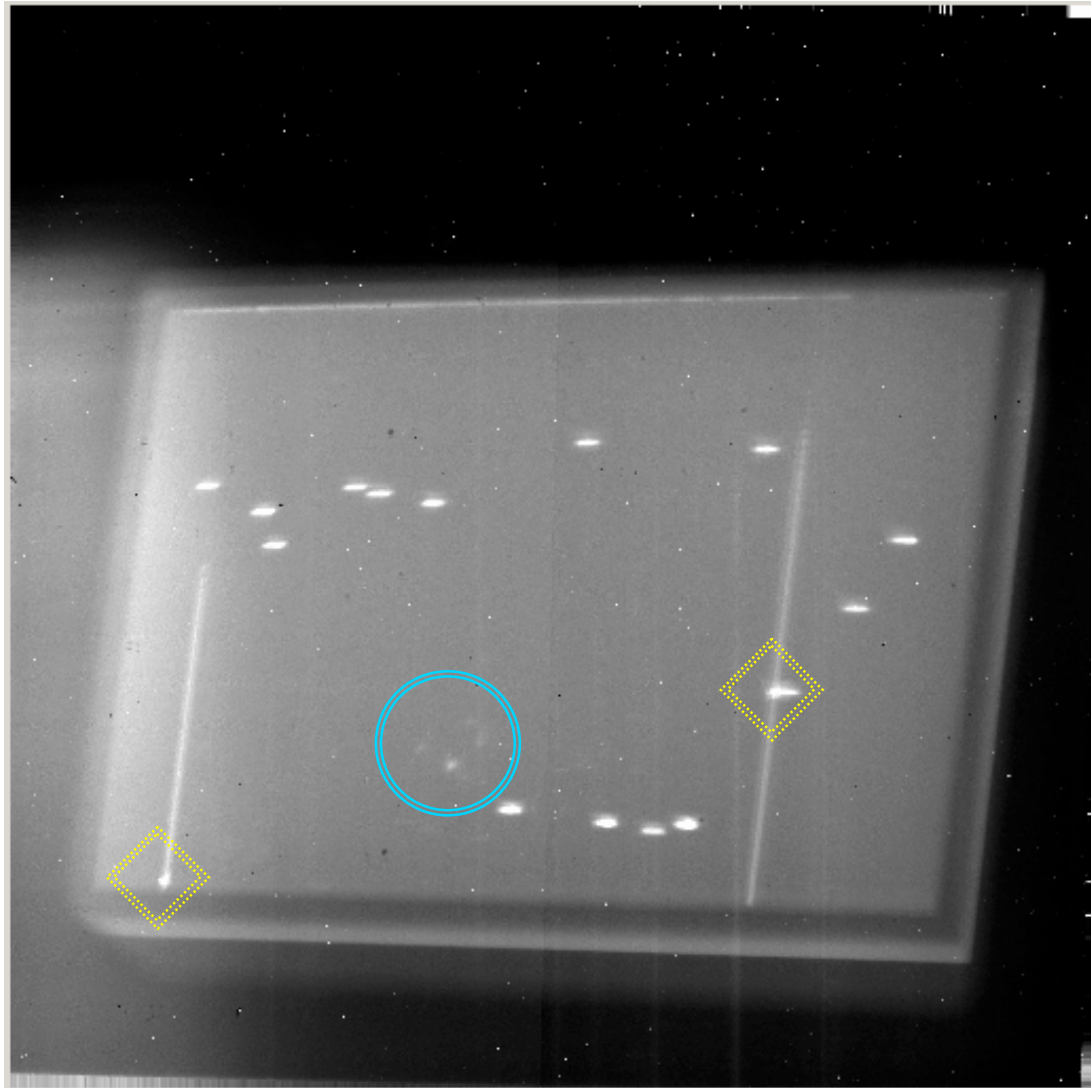


Figure 8. Same as Figure 7, obtained setting the “negative” DMD pattern. Note the LED emitting micromirrors (yellow diamonds) and the leaking Trapezium Stars (cyan circle).

It is important to remark that once the slits have been aligned on the target, they remain aligned regardless on the repeatability of the grating wheel. In other words, the grating wheel can be turned many times, taking spectra at different wavelengths or resolution. The spectra may move around following the vagaries of the grating wheel, but the acquired targets remain well centered, since it is only the telescope pointing who is responsible for maintaining the targets “into the slits”.

The collection of the frame shown in Figure 8 represents the end of the target acquisition process.

7.0 Spectra Acquisition

Once the targets have been acquired, the grating wheel is positioned so to have the selected disperser in the optical path. Figure 9 shows the spectra obtained with the slit pattern shown in Figure 8 setting IRMOS with the Ks band filter, R=3000. The source spectra are visible as vertical lines, whereas the short horizontal lines are due to the OH airglow. The defective mirrors showing LED-type emission produce also a continuum spectrum that may overlap to the spectrum of an astronomical source.

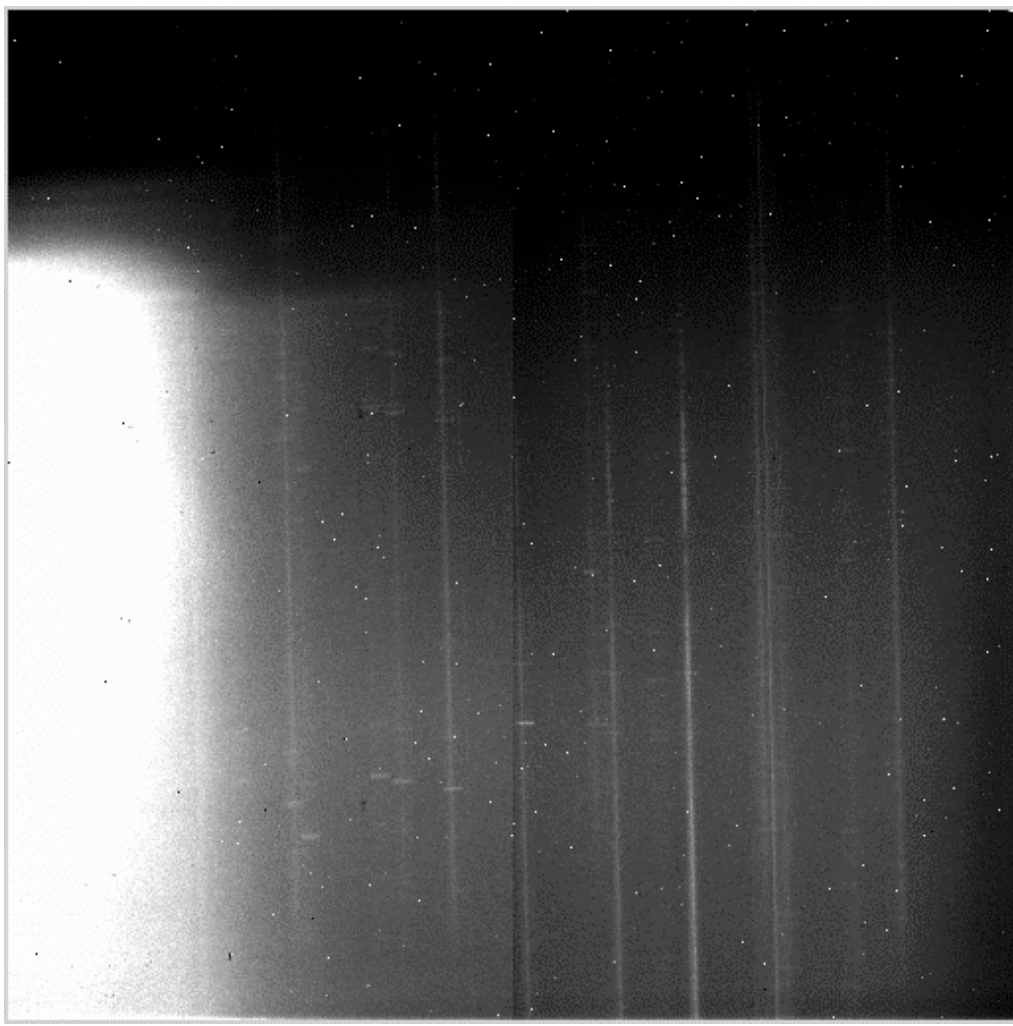


Figure 9. A Ks, R=3000 spectrum of the Orion sources selected with the DMD configuration shown in Figure 8.

Since the position of the grating wheel in IRMOS cannot be accurately controlled, if one moves e.g. to another grating and returns later to the original one, the spectra will turn out to be shifted at different locations (mostly in the vertical direction, since the positioning error is mostly in the dispersion direction). In the same way, if one takes an image, the field will appear shifted in the vertical direction. However, the original alignment of the sources under the slit is never affected by moving the grating wheel.

8.0 Calibration files

In order to extract the spectra, it is necessary to take a number of calibration frames. The strategy envisioned for IRMOS requires three types of calibration images. First, a dark is needed to subtract the dark current, hot pixels and the various sources of extra background, i.e. the thermal emission leaking to the detector and SED-emitting micromirrors. The dark frame, obtained turning OFF all micromirrors, is shown in Figure 10.

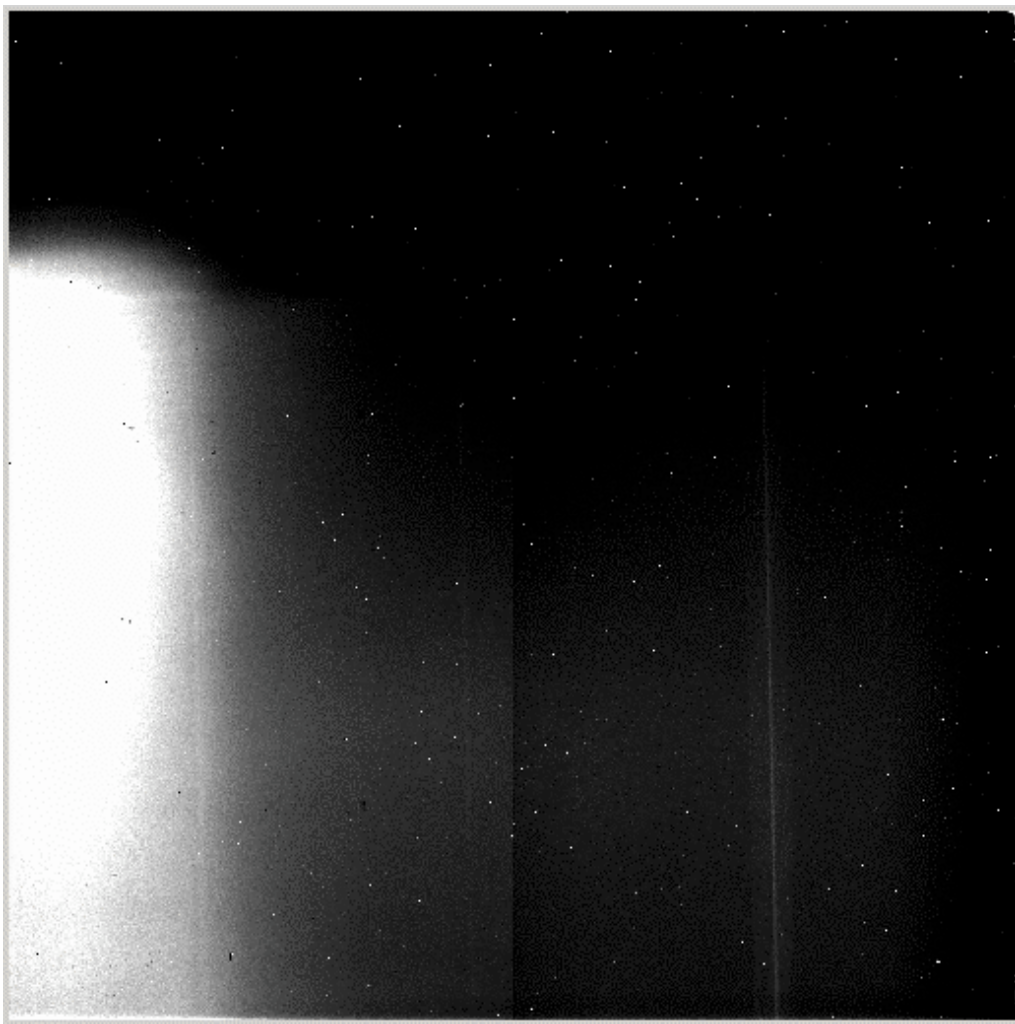


Figure 10. Dark frame obtained by turning off the entire DMD pattern.

The second calibration file is the flat field. In this case, one illuminates with a tungsten lamp the same micromirror pattern used to take the science image. The result is shown in Figure 11.

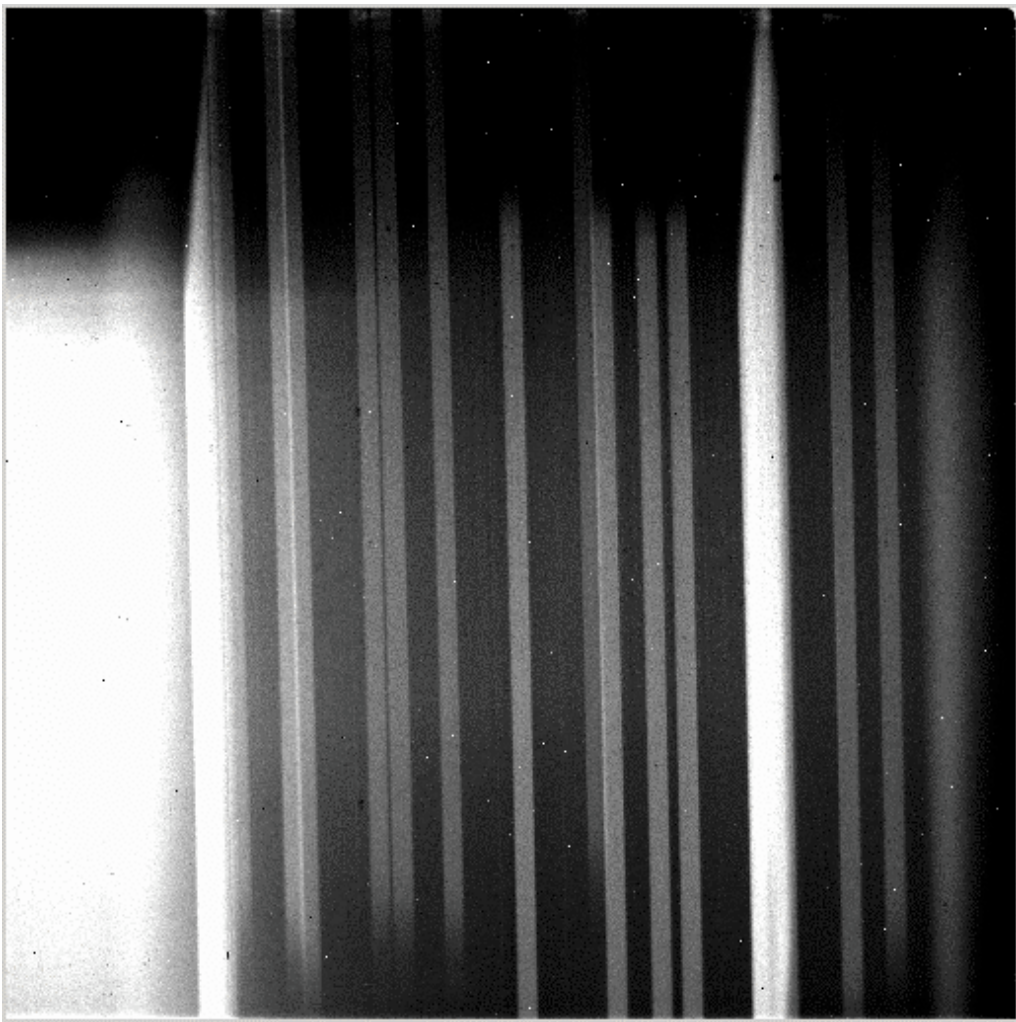


Figure 11. Flat field frame obtained by illuminating the SAME DMD pattern used for science acquisition with a tungsten lamp.

The third calibration file is a new dark appropriate for the flat field. This is necessary because the flat-field is obtained by inserting into the beam a flat folding screen which, while reflecting the light emitted by the tungsten lamp, also emits its own thermal radiation. We therefore take the corresponding dark by simply turning off the tungsten lamp and leaving the screen in the beam, without changing the micromirror pattern. The result is shown in Figure 12.

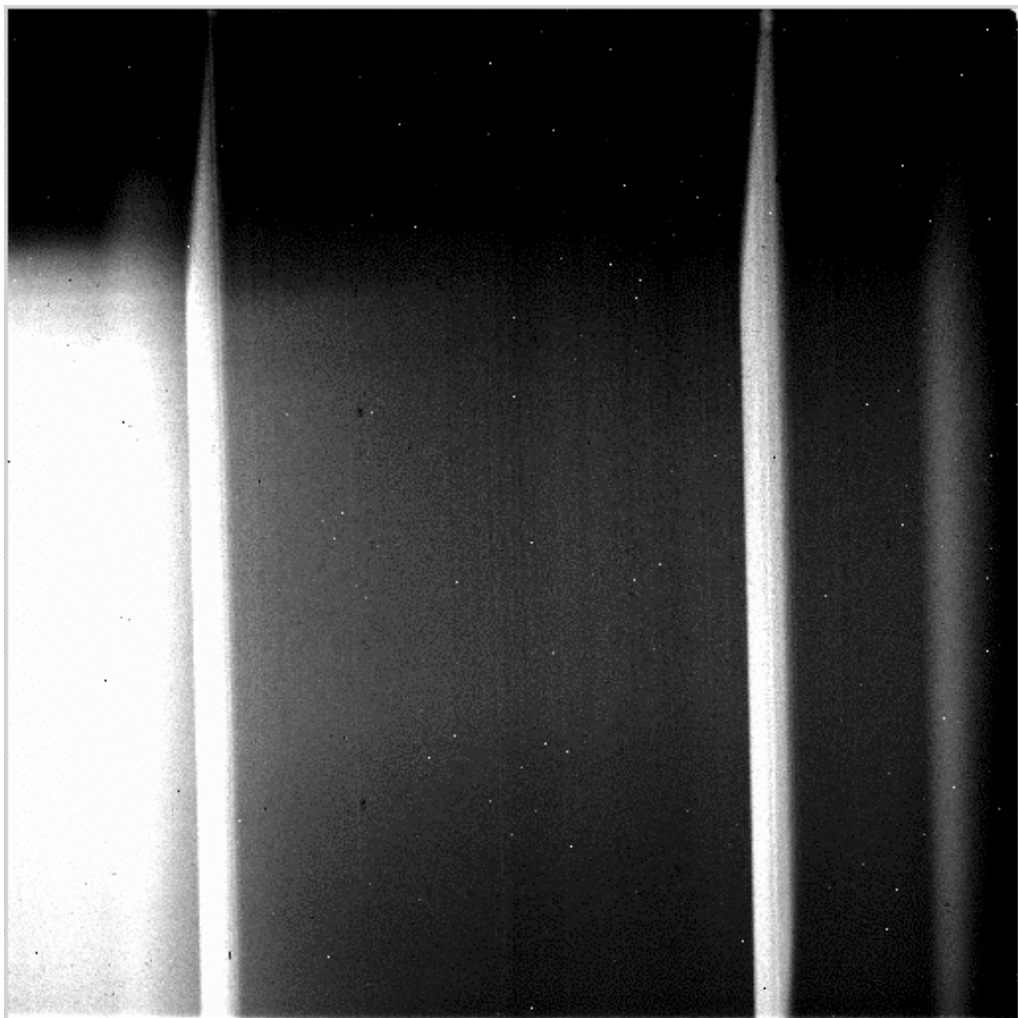


Figure 12 Dark frame appropriate to the flat field illumination.

A comparison of the darks in Figure 12 and Figure 10 shows that the one in Figure 12 has higher diffuse background, most probably due to thermal emission of the screen in the beam.

A fourth frame should also be taken, a line-lamp spectrum for wavelength calibration. This requires the same setup of the flat-field calibration, i.e. the folding screen in the beam, and turning on an arc lamp of known IR spectrum. The same dark used for the flat field can be applied. Due to the similarity between flat-field and wavelength calibration, there is no need to further illustrate this step, also because in the case of IRMOS, as of any other ground based near-IR spectrograph, one can often use the OH airglow spectrum obtained directly on the science images for wavelength calibration.

9.0 A typical observing sequence

From the operational point of view, the typical sequence of events is therefore the following:

1. point the telescope to the field, set the instrument in imaging mode (all DMDs ON, grating wheel in MIRROR position) and acquire the target acquisition image.
2. Select the targets and load the “negative” slits at their position
3. Take a control image and fine tune the slit positions, if needed
4. Revert the slit pattern to the “positive” slit mode, rotate the grating wheel to have the selected grating in the wheel.
5. Take the spectral data
6. Insert the folding mirror and take the dark frames for the flats
7. Turn on the tungsten lamp and take the flat-field frames
8. If needed, take an arc lamp spectrum for wavelength calibration

This procedure assumes that the dark frames for the science exposures can be obtained off-line during day time. Note also that the flat field illumination can be set to flux levels high enough that the amount of time required can be minimal, i.e. a few seconds, without sending the detector in saturation regime.

The procedure we have outlined has minimal impact on the most critical moving parts, i.e. the DMD and grating wheels remain fixed. The main change is turning on and off once per DMD configuration the flat field calibration lamp. A key advantage is that the calibration is done “locally”, with the instrument exactly in the same conditions used to take the science data, without relying on long term stability (which IRMOS does not have) or an instrument model.

10.0 Data Reduction

For IRMOS we have implemented in IDL a simple pipeline performing the following tasks.

For each pointing, i.e. DMD configuration, the science files and the corresponding reference files (dark, flat-field and flat-field dark) are read and stored in IDL data cubes, i.e. arrays of $1024 \times 1024 \times N_{\text{read}}$ elements. The frames of each data cube are averaged together and the two darks frames are subtracted from the relative science and flat-field frames. Cosmic rays and unstable bad pixels are removed as outliers during the data-cube averaging; fixed bad pixels are generally removed by spatial filtering (e.g. a Laplacian algorithm). Figure 13 and 14 illustrate a dark-subtracted science image and the corresponding dark subtracted flat, respectively.

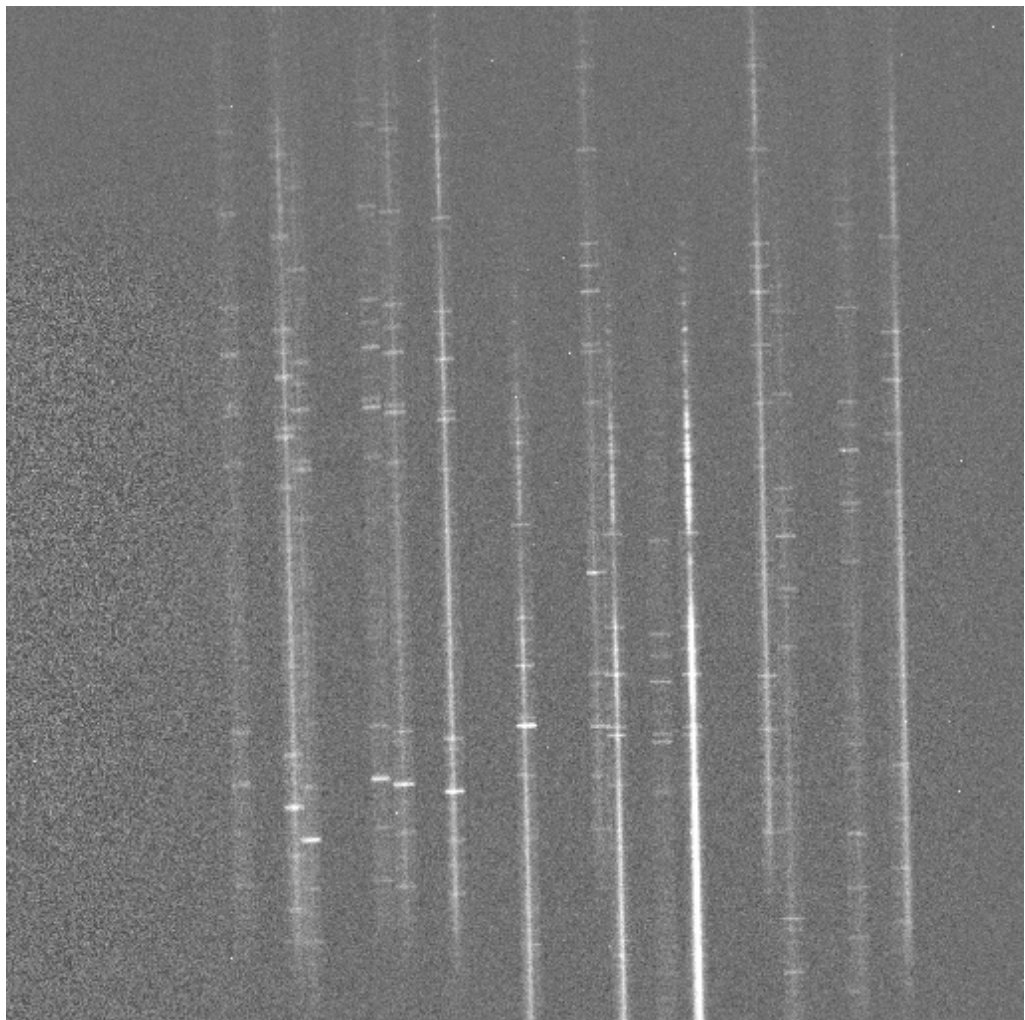


Figure 13 Dark subtracted science image, after bad pixel removal.

Check with the JWST SOCCER Database at: <http://soccer.stsci.edu/DmsProdAgile/PLMServlet>
To verify that this is the current version.

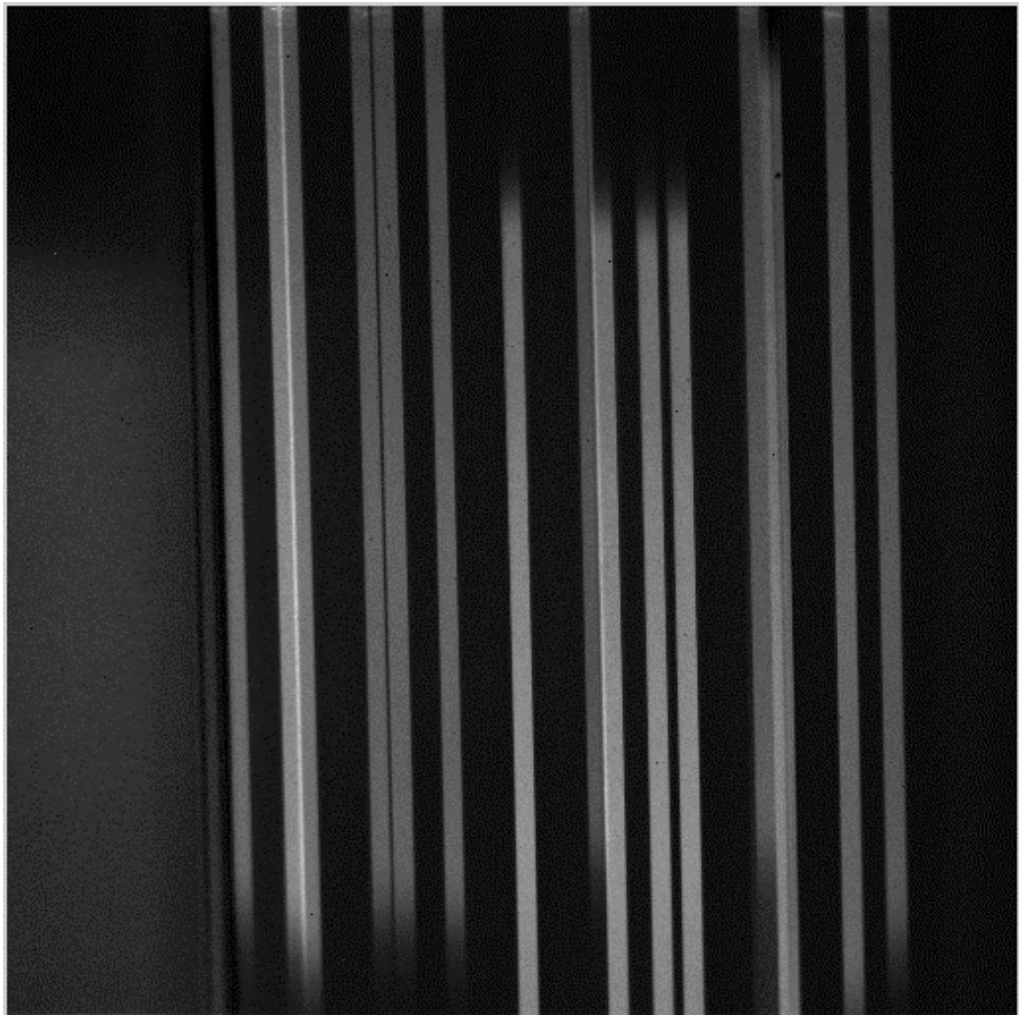


Figure 14. A dark subtracted flat field image, bad-pixel corrected, corresponding to the same DMD pattern and dispersion used to obtain Figure 14.

The science image can then be divided by its flat-field; the result of this operation is shown in Figure 15.

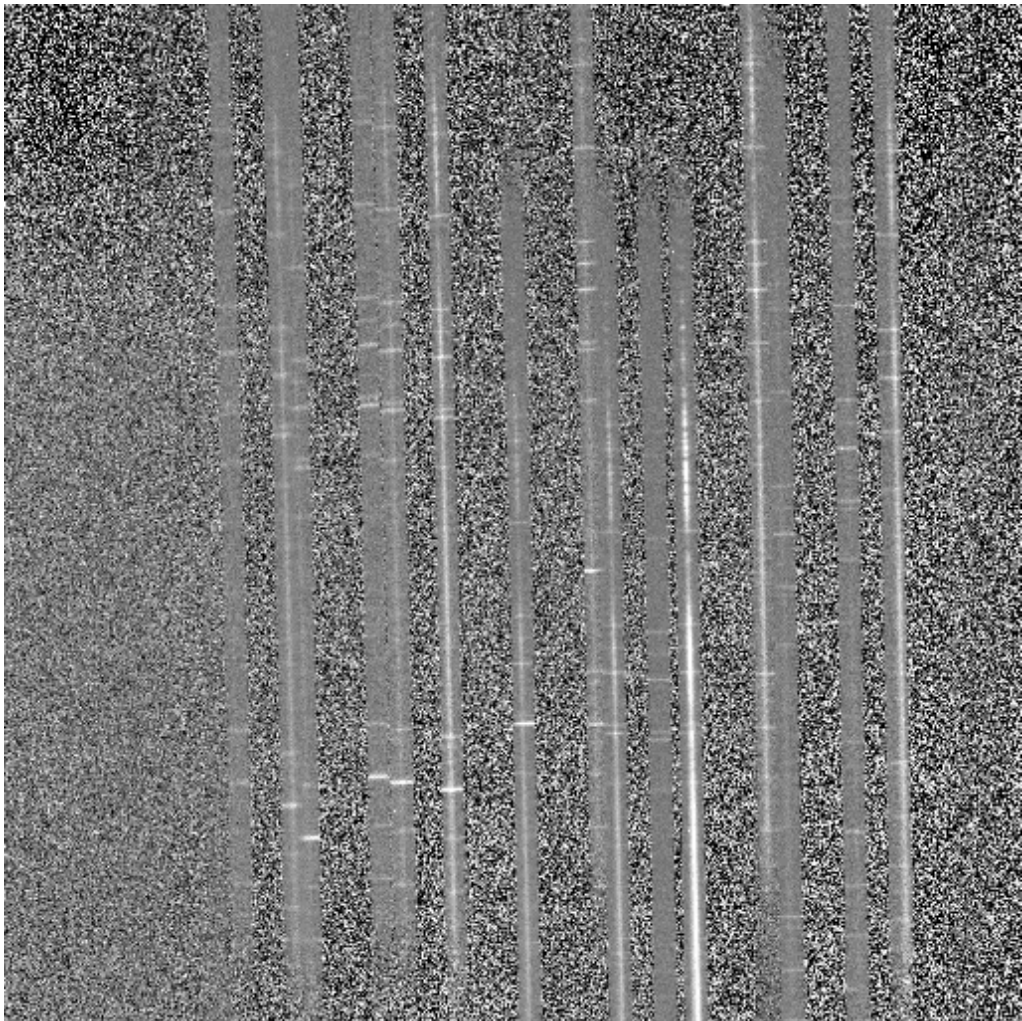


Figure 15. Same as Figure 13, after division by the flat-field in Figure 14.

The spectra are clearly tilted on the field, with an angle in the case of IRMOS of approximately 1.3degrees. To extract the sources out of the individual strips, it is necessary to rectify them. A simple rotation of the field is generally accurate enough for IRMOS. The result is shown in Figure 16.

It is important to notice that the dispersion direction (vertical) and the slit direction (horizontal) do not remain orthogonal across the field, due to the geometric distortion introduced by the spectrograph optics. In fact, once the spectra are vertically aligned, the loci of constant wavelengths, locally defined by the image of the slits in the airglow lines, turn out to be tilted. This is typical in spectrographs with an off-axis optical design, and will affect also the spectra of e.g. NIRSPEC. Figure 17 shows two enlargements of Figure 16, and some variation of the slit tilt angle can already be recognized despite the relatively small distance between the two fields. For this reason, the extraction of the spectra extended over more than one column (as it is always the case with IRMOS) requires the “de-tilting” of the wavelength direction. This is needed not only for the

removal of OH airglow lines, but also of the other background emission due e.g. to the Orion Nebula.

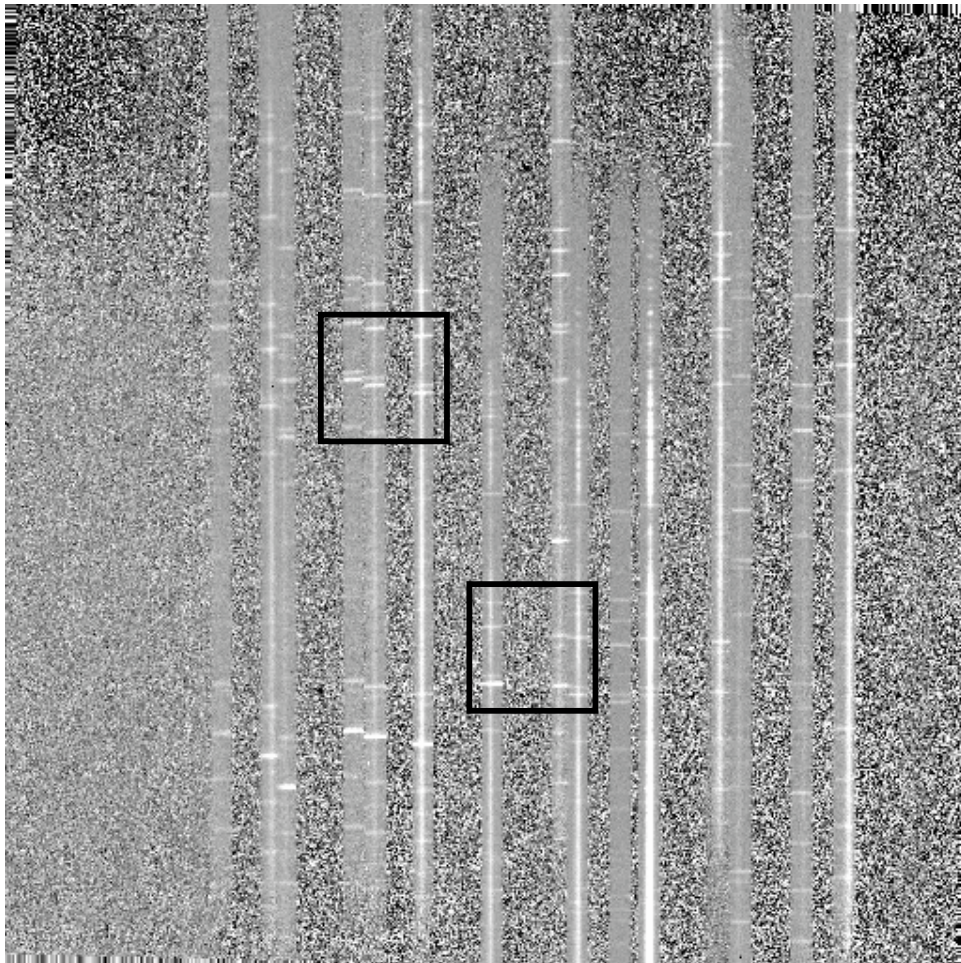


Figure 16. Same as Figure 15, after rotation in the CW direction by 1.3 degrees.

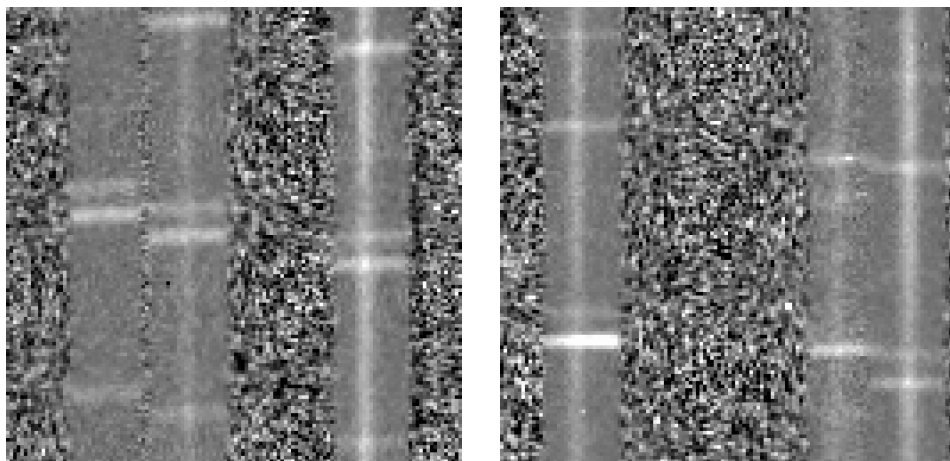


Figure 17. zoom in two regions of Figure 6 illustrating the rotation of the spectral lines.

Once the spectra have been properly aligned in the horizontal and vertical direction, standard spectroscopic data analysis methods are applied. Figure 18 shows the spectra extracted from the observations used in this report, before OH subtraction.

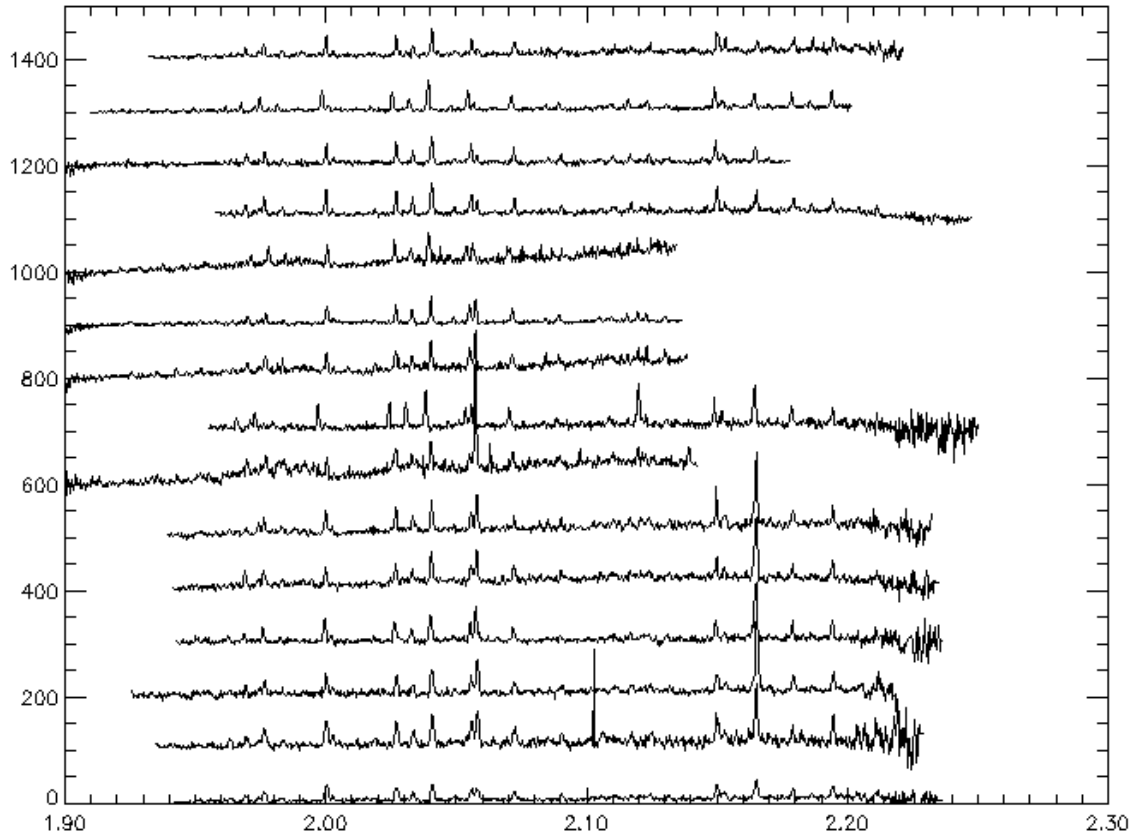


Figure 18. Plot of the spectra extracted from the data set presented in this report. The spectra have not been corrected for OH emission.

11.0 Conclusions

We have illustrated the basic data acquisition strategy of the IRMOS spectrograph, the only existing spectrograph based on MEMS devices. The procedure for taking IRMOS calibration files makes minimal use the critical moving parts, i.e. the DMD and grating wheel, neither relies on instrument models. Having the calibration done “locally”, with the instrument exactly in the same conditions used to take the science data seconds before, enables relatively high level of accuracy regardless on the simplicity of the approach. There are of course substantial differences in instrument requirements, design, performance and operating environment between IRMOS and NIRSPEC. Still, the experience with IRMOS may turn out to be useful for envisioning the NIRSPEC operations, at least in the early commissioning phases, before the full characterization of the instrument.

12.0 Acknowledgements

K. Smith and N. Da Rio participated to commissioning and science runs of the instrument contributing to the definition of the optimal data reduction strategy of IRMOS described in this document.

13.0 References

- MacKenty, J. W., and Stiavelli, M. 2000, ASP Conf. 195, 443
- MacKenty, J.W., et al 2000, ASP Conf. 207, 251
- MacKenty, J.W., et al 2006, SPIE 6269, 626915
- Ohl, R. G., et al. 2003, Proc. SPIE 4841, 677
- Ohl R. G., et al. 2004, Proc SPIE 5492, 1114
- Schepis, J. P., et al. 2003, ESA SP-524, 341
- Winsor R. S., et al. 2000, Proc. SPIE 4092, 102